Origins of perception: retinal ganglion cell diversity and the creation of parallel visual pathways

Dennis Dacey, PhD

University of Washington

Dept. of Biological Structure

National Primate Research Center

Seattle, Washington

Figures: 7

Tables: 1

words text: 7,714

words figure captions: 2,400

Extreme retinal cell type diversity creates parallel visual pathways

The vertebrate retina is a fascinating paradox. On the one hand it is an elegantly simple structure at the periphery of the visual system. Mosaics of receptor cells first 'sample' the retinal image and transduce light to graded neural signals. The photoreceptor signals are then transmitted to a simple circuit of interneurons and an output neuron, the retinal ganglion cell, whose axon projects a representation of the visual world to the brain. On the other hand the retina is a central nervous system structure that has attained an amazing level of neural complexity that continues to challenge neurobiologists (Masland & Raviola, 2000). It is now well understood that the retina contains on the order of 80 anatomically and physiologically distinct neural cell populations (Sterling, 1998; Masland, 2001). The interactions among most of these cell types are precisely arranged in a micro-laminated sheet that provides the architecture for about 20 separate visual pathways (Wässle & Boycott, 1991; Rodieck, 1998; Rockhill et al., 2002).

Each visual pathway originates from an anatomically distinct ganglion cell population and its associated retinal circuitry. The result is a unitary neural structure that gives rise to diverse output pathways with a broad range of distinct visual response properties, from neurons selective for the direction of image motion on the retina (Vaney et al., 2000), to cells with

complex wavelength coding properties used for color vision (Dacey, 1996). Thus with something like a total of 80 neuronal cell populations, used to build 20 visual pathways, the retina represents less a peripheral outpost for transducing light to a few basic visual responses than a major processing stage for the central visual system, and the key to understanding the nature of parallel visual processing.

The retina is a puzzle then whose ultimate solution lies on the other side of the optic nerve in its connection with the brain. What is the impact of recognizing diverse pathways on the rest of the visual system? Specifically how does each ganglion cell population contribute to the key properties of central visual structures and ultimately to visual perception and performance? The goal of this chapter is to begin to address these questions for the primate visual pathway, focusing on our current understanding of the ganglion cell types of the macaque monkey retina and their central connections, physiological properties and possible functional roles.

The reasons for a focus here on the primate are related to a growing awareness, perhaps more than any other part of the visual system, that the retina of an old-world monkey, like a macaque or a baboon, provides a near perfect stand in for its

human counterpart. For example, both human and old world monkey share trichromatic color vision provided by long- (L), middle- (M) and short-wavelength (S) sensitive cone types with virtually the same spectral tuning (Schnapf et al., 1987; Baylor et al., 1987), anatomical organization (Roorda & Williams, 1999; Roorda et al., 2001) and postreceptoral circuitry (Kolb & Dekorver, 1991; Calkins et al., 1994) . As far as has been measured the color vision of macaques and humans is virtually identical (Jacobs, 1993; Jacobs & Deegan, 1997). Thus psychophysical paradigms that define fundamental processes of human vision can be applied to primate retinal neurons to explore underlying cellular mechanisms (e.g. Lee, 1991; Kremers, et al., 1993). Both monkey and man uniquely possess a fovea, the central specialization of the primate retina, where the neural circuitry for high visual acuity resides. Moreover, the many retinal cell types of macaque and human show a close correspondence, even at the level of fine anatomical detail, indicating that the circuitry and physiological properties of macaque retina are surely mirrored in the human (Rodieck et al, 1985; Dacey & Petersen, 1992; Kolb et al., 1992) (Dacey, 1993a; Dacey, 1993b). Finally, recent development of new methods to probe the molecular biology and anatomy of cone photoreceptors (Neitz M & Neitz J, 2003; Roorda & Williams, 1999), as well as the anatomy and physiology of retinal circuitry (Dacey, 1999) has opened the

door to rapid advances in the understanding of primate retinal organization.

Linking diverse ganglion cell types to diverse central targets

At least superficially the diversity of retinal output pathways appears well matched to the diversity of retinal targets in the thalamus and midbrain. Seven main targets, further divisible into at least twenty-four nuclei or layers, receive direct retinal input (Kaas & Huerta, 1988; O'Brien et al., 2001) (Fig. 1). Most of these subdivisions of the visual system in the brainstem have been at least tentatively associated with distinctive and diverse physiological processes. For example, the suprachiasmatic nucleus of the hypothlamus (Fig. 1; SCN) uses retinal input to photically entrain the endogenous circadian rhythm (Berson et al., 2002) while some pathways to the LGN provide signals required for color perception (Merigan, 1989). So a simple hypothesis is that each distinctive ganglion cell population projects in parallel to one or more of the many retinal targets in the brainstem. But previous work suggests that this is largely not the case since the great majority, if not all, ganglion cells project to the superior colliculus and/or the LGN (e.g. Vaney et al., 1981). In macaque monkey for example, it has been estimated that ~90% of the ganglion cells project to the LGN (Perry et al., 1984). Does this mean that

most ganglion cell types project to the LGN? The answer now emerging is yes, most if not all ganglion cell types in primate project to the LGN and/or the superior colliculus. In consequence, the many other smaller targets shown in Figure 1 must therefore receive collateral projections from pathways that also project to these two major structures. In the sections that follow, I will review the evidence for these conclusions by dividing the ganglion cells into two broad groups. The first group is a classically recognized and intensively studied population that exists at relatively high densities. These cells—the midgets and parasols—comprise four distinct types and ~65% of the total ganglion cells. The second group contains more recently identified populations, each population present at relatively low densities. Detailed characterization of this group is only just beginning but it comprises at least 13 distinct types and accounts for much of the remaining 30-40% of the total ganglion cells.

Classical high density pathways to the LGN: midget and parasol cells

The names midget and parasol refer to two anatomically distinct groups of ganglion cells that project respectively to the parvocellular and magnocellular sectors of the LGN (Leventhal et al., 1981; Perry et al., 1984) (Fig. 2A). These two groups share

the common feature of a high to moderate overall spatial density relative to all other ganglion cell types. Indeed, their relative numerosity is the reason that these cells have been the only ganglion cells that were significantly sampled with classical anatomical and physiological methods, and have thus driven most thinking about the functional organization of the primate retinogeniculate pathway (e.g., Kaplan & Shapley, 1986; Merigan & Maunsell, 1993). For this reason midget ganglion cells are often referred to as P-cells and parasol ganglion cells as M-cells to denote their central projection and by implication their visual function.

There have been many detailed reviews that consider the visual roles of midget and parasol ganglion cells (e.g., Shapley & Perry, 1986; Kaplan et al., 1990; Shapley, 1995). Since the LGN is the major thalamic relay for conscious visual perception of form, color and motion it is not surprising that all of these functional roles have been doled out to the midget and parasol ganglion cell types. With the recognition that other ganglion cell types project to the LGN however hypotheses about the functional roles of these pathways must be modified (e.g., Dacey, 1996). In this section I briefly review some of the basic properties of the midget and parasol cells. My purpose here is not to recapitulate the large body of data and hypotheses that

have already been extensively reviewed but to summarize the limits of our understanding concerning the function of these major pathways. I will then argue, in the final section of the chapter, that the identification of novel visual pathways has the potential to solve some longstanding retinal puzzles.

Midget and parasol ganglion cells each comprise two distinct populations whose dendrites stratify in either the inner or outer portion of the inner plexiform layer (IPL)(Watanabe & Rodieck, 1989; Silveira & Perry, 1991; Dacey, 1993b). This inner-outer dichotomy is a major organizing principle that subdivides much of vertebrate retinal circuitry into ON- and OFF-center pathways (Famiglietti et al., 1977). 'Inner' cells receive excitatory input from depolarizing-ON cone bipolar cells and thus show ON-center receptive fields and 'outer' cells are driven by hyperpolarzing-OFF bipolars conferring an OFF-center light response (Dacey et al., 2000). Thus at any given retinal location there are two midget and two parasol cells that respond with opposite polarity to incremental vs. decremental visual stimuli.

The midget and parasol ganglion cell populations show other anatomical features typical of many mammalian ganglion cells. The inner-ON and outer-OFF cells independently and uniformly

tile the retinal surface with their dendritic trees and thereby create separate maps of the visual field with a characteristic central-to-peripheral gradient in cell density. Thus the density of the dendritic 'tiles' composing these two maps changes systematically as a function of retinal eccentricity: in central retina, dendritic trees are small and cell density is high; with increasing distance from the fovea the dendritic tree enlarges and cell density decreases (Fig. 2A). A consequence of this inverse relationship between dendritic field size and density is that the visual map remains seamless but the spatial grain, and thus spatial resolving power, of that map declines in the retinal periphery.

Beyond these similarities, midgets and parasols differ anatomically in two major ways that have been well documented. First, the dendritic field diameters of midget cells are significantly smaller than that of the parasol cells at any given eccentricity (Fig. 2A). Second the two groups stratify at different depths in the inner and outer IPL (Fig. 4). The difference in stratification depth reflects input from distinct cone bipolar cell populations (Wässle, 1999). Thus the parallel nature of these pathways begins at the level of the bipolar cell and its pattern of connections to the L-, M- and S-cone photoreceptors. The degree to which these differences create

functionally distinct pathways is considered for the midget and parasol cells in turn below.

The midget pathway – high density for color opponency, visual acuity or both?

It is well established that in the central 10 degrees of visual angle, the midget dendritic arbor is barely 5 microns in diameter and receives virtually all of its excitatory input from a single, equally small midget bipolar cell which in turn connects to a single cone photoreceptor (Polyak, 1941; Kolb & Dekorver, 1991; Calkins et al., 1994).

Because of this 'private-line' circuit the midget ganglion cells are present at a very high density relative to all other ganglion cell types. In central retina where cone density peaks the midget pathway follows the cone density gradient and there are two midget ganglion cells for every cone (Ahmad et al., 2003). Here the midget populations together constitute up to 70% of the total ganglion cell population (Calkins et al., 1995). In foveal retina the peak density of cones sets the limit on achromatic spatial resolution (Packer & Williams, 2003), and the private line midget circuit is capable of preserving and transmitting this information to the brain (Wässle et al., 1990; McMahon et al., 2000). As already mentioned the midget ganglion

cells project selectively to the parvocellular division of the LGN and lesions of the parvocellular layers reduces visual acuity (Merigan et al., 1991a; Merigan et al., 1991b; Lynch et al., 1992; Merigan, 1996). The conclusion thus seems inescapable that the midget signal functions to preserve the visual acuity afforded by the sampling density of the cone mosaic. Surprisingly however, physiological studies of the visual responses of midget ganglion cells and parvocellular LGN relay cells have strongly emphasized not a primary role for midget cells in achromatic spatial vision but the major role that these cells play in color vision.

Wiesel and Hubel (1966) recognized that the single cone midget pathway might be critical for trichromatic color vision in primates. To extract information about wavelength that can be used for color discrimination the circuits of the visual system must compare the outputs of cone types with maximal sensitivities at different points along the visible spectrum. In trichromatic primates the S-, M- and L-cones, have sensitivity peaks at short, mid and long wavelengths respectively. The midget cell, via its dedicated excitatory connection to a single cone, thus has the potential to compare the excitatory input from one cone type to an inhibitory input from another cone type. Recordings from presumed foveal and parafoveal midget

cells and their parvocellular LGN counterparts support this 'midget hypothesis' of wavelength coding (Figure 2B). Cells that are excited by input from L-cones, tend to be selectively inhibited by M-cones and this L vs M cone signal is referred to as cone-opponency (e.g., DeValois et al., 1966; DeMonasterio & Gouras, 1975; Derrington et al., 1984; Reid & Shapley, 2002). Such cone signal opponency at the level of the retina has an important psychophysical correlate, where cone-opponent transformations are a critical step in the perception of color (e.g., Abramov & Gordon, 1994; Gegenfurtner & Kiper, 2003).

The apparently straightforward anatomy and physiology linking the midget pathway to both achromatic visual acuity and second, to color vision has led to the suggestion that the midget pathway must do 'double-duty'. This hypothesis rests on a center-surround receptive field model in which chromatic stimuli at low spatial frequency engage center and surround and give rise to a strong response while stimuli at high spatial frequencies engage primarily that receptive field center and transmit an achromatic signal (e.g., see Gegenfurtner & Kiper, 2003 for the most recent description of this view). The 'double-duty' hypothesis has not gained universal acceptance however and views about the overall functional role of the midget pathway remain surprisingly contentious. Thus, it has been shown that

the cone opponent, L vs M signal in the midget pathway can seriously degrade the achromatic contrast sensitivity and makes these cells poor candidates for playing any significant role in achromatic vision (Kaplan & Shapley, 1986). To a luminance modulated, achromatic stimulus, like a drifting black and white grating, L and M cones are modulated in phase so that a cell in which these two cone types are antagonistic responds poorly to such a stimulus due to cancellation of the cone signals. In essence the color properties appear to be in direct conflict with the achromatic properties and the mechanism by which both a robust achromatic signal as well as a chromatic signal could be extracted at higher processing levels remains unclear (Kaplan et al., 1990); Shapley, 1995). Consequently it has been proposed that the specialized, private-line midget pathway has evolved specifically to generate a specialized circuit needed to generate L vs M cone-opponency for the purpose of color vision (Shapley & Perry, 1986; Lee, 1999).

At the same time the fundamental role of the midget pathway in color-coding has also been challenged (Rodieck, 1991; Calkins & Sterling, 1999). Although recent results argue that midget ganglion cells receive cone-type selective inputs to both the excitatory center and inhibitory surround, just what might be predicted for a specialized color-coding circuit (Martin et al.,

2001; Reid & Shapley, 2002), other results find the chromatic properties of midget cells more variable (Diller et al., in press). Moreover, both physiological and anatomical studies of the retinal circuits that create the inhibitory surround have not been able to uncover any cone type specificity in retinal inhibitory pathways (Calkins & Sterling, 1996; Dacey et al., 1996). Finally, the discovery of another non-midget ganglion cell type that transmits highly specific S cone-opponent signals (Dacey & Lee, 1994) has focused attention on the role that other novel ganglion cell types might play in color vision.

In summary, it is quite remarkable that three distinct hypotheses—covering the complete range of the possibilities about the function of the midget pathway—have all been forcefully argued. First, that the midget pathway is uniquely specialized for color vision (e.g., Reid & Shapley, 2002); second, that the midget cells are uniquely specialized for achromatic spatial vision and set the limit on peak visual resolution (e.g., Calkins & Sterling, 1999) and third, the middle ground, that the midget pathway does 'double-duty' and is a critical component of both achromatic and chromatic vision (Lennie, 2000). Though this last hypothesis in principle is parsimonious it remains to be shown that the midget ganglion cell receptive field consistently functions in this manner.

Parasol pathways — moderate density and high achromatic sensitivity

By contrast with the midget ganglion cells the parasol ganglion cells show larger dendritic fields and are narrowly stratified near the center of the IPL. Each parasol population constitutes 5-8% of the total number of ganglion cells in mid-peripheral retina. Unlike the midget pathway the parasol cells receive input from multiple cone bipolar cells with larger dendritic fields that receive synergistic input from multiple L and M cones (Calkins, 1999; Jacoby et al., 2000; Jacoby & Marshak, 2000; Marshak et al., 2002). As a result, parasol cells respond strongly to achromatic or 'luminance' stimuli in which L and M cones are modulated in phase and more weakly to a isoluminant modulation in which L and M cones modulate in counterphase (Fig. 2B). Because parasol cells project to the magnocellular layers of the LGN they are considered to be the major, if not sole source, of the achromatic signal that is relayed from the magnocellular layers to primary visual cortex. However it is important to note that parasol ganglion cells also project to the superior colliculus (Leventhal et al., 1981; Perry & Cowey, 1984), Dacey, unpublished observations). Parasol cells consistently show a very high sensitivity to achromatic contrast, much higher than that of midget cells to the same

stimuli (Kaplan & Shapley, 1986). For this reason it has been argued that the parasol-magnocellular pathway may be the main signal for achromatic spatial vision (Lee, 1999). This role for the parasol cells would be consistent with the proposal that the midget system is uniquely specialized for color vision. The relatively low density of these cells, relative to midget cells in foveal retina seems to argue against such a primary role, however. More strikingly lesions of the magnocellular layers of the LGN show a loss in achromatic vision at low spatial frequencies but not at the high spatial frequencies presumably supported by the midget pathway (Merigan & Maunsell, 1990).

Parasol cells, by virtue of their projection to the magnocellular layers of the LGN have also been implicated as the retinal origin of signals used to create direction selectivity at the level of visual cortex that reflect the first stage in a parallel pathway for motion perception. However lesions of the magnocellular pathway, while reducing visual capacity, do not effect motion perception specifically (Merigan et al., 1991a). In this regard it is important to recognize that direction selectivity is a well established property of certain mammalian retinal ganglion cells and before reaching any strong conclusions about the role of the parasol cells in motion processing it will be necessary to fully assess the physiology

and central projections of the remaining primate ganglion cell types.

In sum, parasol ganglion cells are clearly implicated as an important achromatic pathway, but the precise visual role these cells play relative to the midget ganglion cells and other ganglion cell types remains to be established.

Novel pathways to LGN and superior colliculus: 13 low density types

While the specific functional roles of both the midget and parasol pathways remain unsettled, the recognition of ganglion cell diversity raises a number of new and relevant questions. How many other ganglion cell types contribute to the retinogeniculate pathway? How many participate in chromatic signaling? How many other types are clearly achromatic? Are there any types that are explicitly implicated in motion processing, i.e., show direction selectivity?

The midget and parasol ganglion cells together constitute over half the total ganglion cells, yet are but a fraction of the total ganglion cell types. Outside of the fovea, where relative densities can be easily calculated, these cell groups account for about 50 to 65% of the total, depending on retinal location

and estimates of local cell density (Table 1). The number of remaining ganglion cell populations depends entirely on the relative density of each distinct group.

As will be shown below the majority of mammalian ganglion cell types exist at relatively low densities, ranging from less than 1% to about 5% of the total. Because of this basic feature of retinal organization these low-density types have been extremely difficult to identify and characterize with standard physiological and anatomical methods. Low-density cells are rarely if ever sampled by the 'blind' electrode of the physiologist or anatomical labeling methods. However, application of techniques directed at overcoming this natural bias have quickly revealed the true extent of retinal cell diversity. The emerging picture for primate retinal ganglion cells is summarized below; recent results for rodent (Sun et al., 2002) rabbit (Rockhill et al., 2002) and cat (Isayama et al., 2000) reveal the same basic picture.

Small bistratified ganglion cells – a non-midget pathway for color vision

The first real glimpse of ganglion cell diversity in primate came from experiments using an intact in vitro preparation of the human or macaque retina in which either vital staining or retrograde

labeling from central tracer injections were used to target individual ganglion cells for intracellular staining (Watanabe & Rodieck, 1989; Dacey, 1989; Rodieck & Watanabe, 1993a; Dacey, 1993a; Dacey, 1993b) Peterson & Dacey, 1998; Peterson & Dacey, 1999; Peterson & Dacey, 2000). The results of these studies illustrated several morphologically distinct groups whose physiological properties were unknown. Among these cells was a distinctive bistratified ganglion cell population that was retrogradely labeled from tracer injections in the LGN and showed a dendritic tree size comparable to that of the parasol ganglion cell (Dacey, '93; Rodieck & Watanabe, 1993) (Figure 2A). Estimates of the density of the small bistratified cells suggested that they compose about 5% of the total ganglion cell population (Dacey, 1994). The dendritic tree, stratified narrowly in both the inner and outer part of the IPL suggested that these cells would receive input from both ON and OFF cone bipolar pathways. These results stimulated the further development of the macaque in vitro preparation to enable intracellular recording and staining methods to be used to directly link the bistratified morphology to visual receptive field properties (Dacey & Lee, 1994).

Recordings from the small bistratified cells in vitro revealed a strong excitatory ON input from the short wavelength sensitive S cones that was opposed to an inhibitory input from L and M cones

(Figure 2B). This type of S cone-opponent response had been classically observed by extracellular recording methods at both the level of the retina and LGN as part of the midget-parvocellular pathway and recognized as one of the major axes of opponent color space that is utilized for higher order color processing (e.g., Derrington et al, 1984). Using the same stimuli it was also shown that such S-cone input was apparently lacking from identified midget and parasol ganglion cells that were also recorded from in the in vitro preparation (Figure 2B). Most recently evidence has been given that the small bistratified cells project to a restricted locus at the border between the magnocellular and parvocellular layers in or near koniocellular layer 3 (Martin et al., 1997; Hendry & Reid, 2000). The small bistratified ganglion cells thus represent a parallel pathway for S-cone related color signals completely independent of the midget pathway.

Detailed study of the synaptic organization of this pathway reveals a distinct circuitry in which S-cone signals are transmitted to the inner dendritic tier of the small bistratified cell by a cone bipolar cell that makes selective connections with S-cones (Calkins et al., 1998). The precise mechanism for the strong S vs L+M cone opponency remains to be fully worked out but is likely to arise in the center-surround

organization of the S-cone bipolar cell (Dacey, 2000) and by antagonistic L+M cone input via OFF cone bipolar cells connections to the bistratified dendritic tree (Calkins et al., 1998).

Our understanding of S-cone pathways and their full role in color vision remains incomplete. As will be shown below, other novel ganglion cell types transmit S-cone opponent signals to the LGN. It has also been shown that OFF midget bipolar cells contact S-cones providing a potential midget pathway for S-OFF signals in the foveal retina (Klug et al., 1993).

Retinal fireworks display remaining low-density ganglion cell types

The identification of the small bistratified cell as a previously unrecognized color-coding pathway initiated the systematic investigation of the remaining ganglion cell populations with the goal of making the link between central connections, morphology and physiology for novel retinal ganglion cell types using the in vitro preparation of the macaque retina. To achieve such a goal retrogradely labeled ganglion cells can be successfully targeted for intracellular recording and staining in vitro. Reliably targeting a specific cell, especially a low-density type, is extremely difficult with

this method however. This is because little morphology is revealed after retrograde labelling to permit specific cell types to be consistently identified and studied both anatomically and physiologically; progress is therefore extremely slow. Recently however, a tracing method—discovered by serendipity—has revealed the complete morphology of large numbers of retrogradely labeled cells in vitro and has quickly and efficiently unveiled a more complete picture of primate ganglion cell morphology (Dacey et al., 2003) . The method, termed retrograde photodynamics, relies on the tracer rhodamine-dextran. When ganglion cells retrogradely labeled with this tracer are observed in vitro they show the typical granular accumulation of tracer in the cell body. However, when these cells are observed with epifluorescent illumination the sequestered tracer is liberated into the cytoplasm, in a striking firework-like display. The tracer quickly diffuses throughout the dendritic tree revealing the complete dendritic morphology of the retrogradely labeled cell (Figure 3). The exact mechanism by which light leads to the release of the sequestered fluorophore is not known, though it is likely that rhodamine acts as a photosensitizing molecule in which excitation of the fluorophore by light leads to the creation of reactive oxygen species which in turn damage the cellular structure that is locally concentrating the fluorophore.

The anatomical picture now emerging from retrograde photostaining after rhodamine-dextran injections placed in LGN and superior colliculus illustrates the characteristic mammalian pattern of extreme cell type diversity. Including the small bistratified cell, a total of 13 novel types have been clearly identified, and with further analysis this number may grow to at least 17. Two views of the morphological details are illustrated in Figures 4 and 5. For discussion purposes, the retrogradely labeled cells can be divided into six new groups based on one or two shared, basic features of dendritic morphology. Each ganglion cell population within the group can be further distinguished by stratification pattern in the inner plexiform layer (Figure 4B).

Thorny cells

The 'thorny' cell group is characterized by a moderately large field of dense branching fine caliber dendrites that are studded with small thornlike extensions (Fig. 5). These thorny cells can be further divided into three types by depth of stratification in the IPL; the broad thorny, with a thicker dendritic tree in the center of the IPL and two other types, narrowly monostratified near the inner and outer borders of the IPL (Figure 4A and 4B). Both the broad thorny and narrow thorny

cells have been retrogradely labeled from the superior colliculus and the LGN (Rodieck & Watanabe, 1993b; Dacey et al., 2003) . Complete cell counts of the thorny populations is not yet possible but the relative spatial density of each type can be estimated from measurements of dendritic field diameter and observations of the local spacing of neighboring cells of the same morphological type from photostained retinas. At any given eccentricity the thorny cell types show a dendritic field overlap characteristic of most ganglion cells types (coverage of about 1-2) but show about twice the dendritic field diameter as neighboring parasol ganglion cells. Based on total ganglion cell counts, each thorny population would account for about 1% of the total ganglion cell population in mid-peripheral retina (Table 1).

The thorny cells have not yet been physiologically characterized in detail but initial recordings of these cells in vitro suggests that these cells give transient light responses and are not direction selective. The broad thorny cells, as expected from a dendritic morphology that straddles the ON-OFF border at the center of the IPL, show a transient ON-OFF response but also without the direction selectivity that is present in certain transient ON-OFF cells of other mammalian retinas. Nothing is currently known about the cone inputs to these cells or their

possible roles in chromatic or achromatic visual pathways that reach the level of visual cortex or extrastriate cortex.

Recursive cells — Direction selective circuits in primate retina?

The recursive group shows moderately densely branched trees in which many secondary dendritic branches have a strong tendency to curve back toward the cell body and in some instances form closed loops of apposing, recursive dendrites (Figure 5). Another feature of these cells is that even though the dendritic fields are large, neighboring cells are very closely spaced giving rise to a high degree of dendritic overlap; moreover the overlapping dendrites of neighboring cells have a tendency to entwine and run together in dendritic fascicles. The recursive cells can be divided into a bistratified group, with separate strata near the center of the IPL and a single monostratified group with stratification in the inner portion of the IPL where ON-center cells are expected to stratify (Figure 4A and 4B). Both groups of recursive cells have been retrogradely labeled from tracer injections into the superior colliculus; in one instance the monostratified group was labeled from injections placed into the LGN.

The recursive cells have not yet been recorded from but their anatomical profile nicely fits the picture for the two major groups studied in great detail in rabbit retina – the ON and ON-OFF direction selective (DS) cells (Vaney et al., 2000). First, the recursive branching is a characteristic feature of both ON and ON-OFF cells. Second, the high dendritic overlap, and dendritic co-fasciculation is also observed for rabbit direction selective cells; in rabbit this reflects the subdivision of this group into several distinct types. Each type tiles the retina independently with little dendritic overlap and shows a characteristic directional preference. Thus, in rabbit there are 3 ON DS types and 4 ON-OFF DS types. It therefore seems likely, though not yet shown conclusively, that a similar picture of 7 directionally selective types will hold true for macaque and could prove to be an important early signal for motion processing pathways in the primate visual system.

Large bistratified cells – a new S-ON chromatic pathway

The large bistratified cells are present as a single population that is consistently labeled after tracer injections into the LGN (Figure 5). These cells, like the small bistratified cells show two strata near the inner and outer IPL borders, with the inner dendritic tier in the vicinity of the known stratification of the axon terminal of the S-cone selective cone bipolar cell

type (Figure 4A and 4B). The large bistratified cell shows a more sparse branching pattern and larger dendritic field diameter than the small bistratified cells (Figure 5). Dendritic field diameter and observed overlap suggest that these cells compose about 3% of the total ganglion cell population in mid-peripheral retina (Table 1). However, in foveal retina the large and small bistratified cells appear similar in size (Dacey et al., 2003) , so like the midget ganglion cells, the relative density of this cell group may increase in central retina.

Strikingly, the first recordings from large bistratified cells revealed a clear excitatory input from S-cones together with inhibitory input from L and/or M cones and thus provide a second anatomically distinct S-ON opponent pathway to the LGN (Fig. 6B). At first glance the light response of these cells appears much like that of the small bistratified cells but detailed information about the relative signs and strengths of the L, M and S-cone inputs to the receptive field and an overall understanding of the spectral sensitivity of this cell type will be needed before any conclusions can be drawn about the role of this pathway in chromatic processing.

Sparse monostratified cells – an S-OFF chromatic pathway

This group shows large and narrowly stratified dendritic trees like the smooth monostratified cells but much more sparsely branching (Figure 5). Two populations are stratified close to the outer and inner border of the IPL (Figure 4). These cells are also consistently labeled from tracer injections into the LGN and initial recording from this type revealed yet another type of S-cone opponent in which the S-cone input is inhibitory and opposed by an excitatory input from combined L and M cone input. (Figure 6A).

S-OFF opponent responses have been recorded at the level of the LGN and primary visual cortex and an S-OFF signal is a well established, psychophysically characterized component of opponent processing in human color vision (e.g., DeValois et al., 2000; Knoblauch & Shevell, 2001; Monnier & Shevell, 2003). However since all known S-cone related circuitry derives from an excitatory ON pathway to the inner part of the IPL, S-OFF responses recorded at higher levels are usually assumed to reflect more central processing of the S-cone signal (DeValois et al., 2000; DeValois et al., 2000). Our current understanding of this pathway in relation to the S-ON circuitry is limited and the source of the S-OFF signal is unclear. No S-cone selective OFF-bipolar cells have been identified as a counterpart of the

S-ON bipolar and the large sparsely branching dendritic trees of the S-OFF ganglion cells are stratified in the inner portion of the inner plexiform layer, where S-ON-pathway signals are transmitted. Either the inhibitory S-signal reaches this cell by a sign inversion of the S-ON bipolar signal or the S-cone signal is in some way introduced to the inhibitory surround of this cell. Future measurements of receptive field structure together with pharmacological manipulations of ON and OFF signals will be needed to address this question.

Smooth monostratified cells – alpha-like cells of the primate?

By contrast with the thorny group the 'smooth monostratified' types are larger in dendritic field diameter, show thicker caliber radiate and thornless dendrites and form an inner and outer cell pair that are narrowly stratified near the center of the IPL, very close to but not overlapping with the stratification of the parasol cells (Figures 4 and 5). Also like the parasol cells the smooth monostratified cells have relatively large cell bodies and are retrogradely labeled from both the superior colliculus and LGN. Together the inner and outer populations probably account for about 2-3% of the ganglion cells in the mid-retinal periphery (Table 1).

This cell group has not yet been recorded from but anatomically they are comparable to the intensively studied alpha cell of cat retina (Peichl, et. al, 1987). It is therefore possible that these cells are comparable to the alpha-Y cell pathway. Previous studies have offered conflicting opinions about the primate correlate of the Y-cell system. If the primate retina is considered as giving rise to just two major functional retinogeniculate pathways, then the parasol-magnocellular projecting ganglion cells appear to correspond to the cat alpha-Y as the origin of signals that contribute to early motion processing (Rodieck, et al., 1993). At the same time it has been shown that the magnocellular layers contain cells that show both linear (X-cells) and non-linear spatial summation (Y-cells) suggesting multiple functional pathways project via the magnocellular layers (Shapley & Perry, 1986; Kaplan et al., 1990). Clearly, the existence of some number of novel ganglion cell types projecting to the LGN now opens the door to a revisiting this question in the future.

Giant monostratified cells – a pupillomotor, irradiance coding pathway

These cells have been consistently labeled from tracer injections into the LGN and the pretectal olivary nucleus (PON) (Gamlin et al., 2001; Dacey et al., 2003). They show extremely

large, and very sparsely branching dendritic trees, that easily distinguish these cells from all other anatomical groups (Figures 4 and 5). The PON is the well-established central relay for visual signals that drive the pupillary light reflex and small tracer injections made into the PON can label the giant monostratified ganglion cells selectively, implicating these cells as the pupillomotor retinal output pathway. The unusual physiological properties of these cells are consistent with this role.

Intracellular recordings from giant monostratified ganglion cells reveal an extremely regular maintained discharge that increases monotonically with increasing background illuminance (Gamlin et al., 2001). The ability of these cells to uniquely code for irradiance is transmitted to the PON (Gamlin et al., 1995; Zhang et al., 1996) and is a key physiological property required to link a fixed pupil diameter to a given irradiance level (Gamlin et al., 1998).

Intrinsic photosensitivity is the basis for irradiance coding by the giant monostratified ganglion cells

The unique irradiance coding by the giant monostratified ganglion cells was paradoxical given that a fundamental property of retinal physiology, beginning with the cone photoreceptors

themselves, is the converse: a rapid reduction in sensitivity to increasing background levels that permits retinal cells to adapt to a wide range of irradiance levels. However recent results have now revealed that the basis for this irradiance coding property lies in the presence of a novel photopigment present exclusively in the giant monostratified ganglion cells themselves. The characterization of this property in the giant monostratified cells has led to a more detailed picture of the anatomy, physiology and central connections of this pathway. It is thus worth considering these results in some detail as an example of the first low-density ganglion cell type in primate to be characterized in detail.

First discovered in rat retina, photoreceptive ganglion cells quite surprisingly responded to light in the absence of all input from rods and cones. These intrinsically photosensitive ganglion cells provided a neural basis for previous observations that a novel photopigment residing in the mammalian eye was capable of entraining the circadian pacemaker of the hypothalamus and also of driving the pupillary light reflex. Thus mice lacking all rods and cones retain circadian rhythms and residual pupil reflex driven by a novel photopigment with peak sensitivity at ~480 nm. The light response of intrinsically photosensitive rat ganglion cells is also mediated by a novel photopigment – with a peak sensitivity ~480 nm. These cells contain

melanopsin, an opsin-like protein, that has become the candidate photopigment, and they project to the suprachiasmatic nucleus and to the pupillomotor pretectum. The intrinsic light response is extremely slow and sustained and permits coding of gross changes in light intensity.

The link between the rat melanopsin-containing, photoreceptive ganglion cells and the giant monostratified pupillomotor ganglion cells occurred with the development of an antibody to human melanopsin. The melanopsin-containing cells were targeted for intracellular recording in vitro by retrograde photostaining from tracer injections into either the LGN or pretectum. Ganglion cells that were retrogradely stained and also melanopsin immunoreactive corresponded to the giant monostratified ganglion cell group that stratified at the extreme IPL borders (Fig. 4A, B). There are about 3000 melanopsin-containing ganglion cells in macaque and human retina - that is only ~2 tenths of one percent of the total ganglion cell population (Fig. 7A). These cells peak in density around the fovea — about 25 cells/mm^2 - where extremely large dendritic trees spiral around the foveal pit. In the periphery there are only a few cells/mm^2 but a loose meshwork of completely stained dendritic processes carpet the retina (Figure 7A).

Melanopsin-containing cell bodies are present in both amacrine and ganglion cell layers and give rise to a distinctive bistratified dendritic plexus situated at the extreme inner and outer borders of the IPL (Figure 7A). Macaque melanopsin-containing ganglion cells show a robust ON-sustained cone driven response to long wavelength stimuli (Fig. 7B). But the use of cone-isolating stimuli shows that these cells are also a second type of S-OFF color opponent ganglion cell with large, coextensive S-cone inhibitory and L+M cone excitatory receptive field components (Fig. 7C). Not surprisingly, given the cone driven light response, these cells also show an equally large rod driven ON input under dark adapted conditions.

Because of the strong cone input to these ganglion cells the intrinsic light response could only be observed in isolation after the application of L-AP4(APB) and CNQX to block glutamate transmission from outer to inner retina. When isolated in this way the intrinsic light response shows the same surprisingly long response latency and slow turnoff observed in rat (Fig. 7D). The spectral tuning of the intrinsic light response is, like the rat, best described by a retinal-based pigment nomogram with a peak at 483 nm (Figure 7E). These ganglion cells thus contain a single novel photopigment – possibly melanopsin – that binds retinal and shows spectral peak situated between the S-cone and the rods.

Other experiments show that in macaque the intrinsic response is present at photopic levels and combines with the cone response. Adding the intrinsic response to the cone response achieves higher spike rates that increase with increasing irradiance. The ability of these cells to show a spike rate that is monotonically related to irradiance is thus created in normal physiological situation by the combined cone and intrinsic signal over much of the photopic range.

In sum, melanopsin-containing cells in macaque show sustained light responses driven by rods and cones and over the full scotopic-photopic range. The cone mediated response shows an S-OFF type of color opponency. The cone response is summed with the intrinsic response over most of the photopic range. The significance of the S-cone opponency is not clear. Since these ganglion cells can be retrogradely labeled from the LGN it is possible that they transmit a cone-opponent signal that participates in color processing. A second possibility is that color opponency may contribute to circadian regulation by providing information about large spectral changes at dusk. Thus Foster and Hefrich-Forster (2001) have speculated: “If the circadian system was capable of using multiple photopigments to ratio changes in the relative amounts of short and long wavelength radiation and of coupling this information with irradiance levels, then the phase of twilight could be determined very accurately.”

Remaining types: Ganglion cells with axon-collaterals, and others

Based on estimates of the total number of macaque ganglion cells and estimates of the relative densities for each ganglion cell type identified thus far, the great majority, certainly at least 90%, of the ganglion cells have been accounted for. It is likely however that other low density ganglion cell populations are present that will be revealed by further tracer injections into central targets. One example is a distinct cell type which shows intraretinal axon collaterals that terminate in the IPL (Fig. 5). Such intraretinal axon collaterals are not a typical feature of retinal ganglion cells and the functional significance of such ganglion cell feedback to the inner retina is not clear. These axon-collateral bearing ganglion cells have been intracellularly stained in both human and macaque retina and a correlate of this cell type has also been observed in both cat and turtle retina (Dacey, 1985; Peterson & Dacey, 1998).

Summary and Conclusions

A broad picture of the primate ganglion cell population can now be sketched, though many critical details of structure and function remain to be added. Diverse ganglion cell populations create many parallel pathways, but it appears that virtually all of these pathways converge on the two major visual structures of

the brainstem, the LGN and superior colliculus, with many ganglion cell types likely projecting to both of these targets. Thus, even though there are on the order of a dozen distinctive smaller retinal targets it must be concluded that most, if not all of these smaller structures receive collateral input from ganglion cell types that project to LGN and superior colliculus; a major question for the future concerns the roles that this complex set of inputs play in the function of the geniculocortical and collicular pathways.

The diverse low density ganglion cell populations sacrifice spatial grain to represent fine detail in the visual image but gain the advantage of a large number of functionally distinct pathways at little cost to the bottleneck of the optic nerve — put simply, the retina can do a lot with a little. This is especially true when considering that the ganglion cell axons, once projected into the brain, can easily collateralize to multiple targets and their signals can be greatly amplified by mechanisms as simple as anatomical variation in the number and density of synaptic boutons in the terminal arbor of the axon. In other words, a low density of ganglion cells in the retina need not be an indication of the strength of the signal centrally. The strategy of doing a lot with little is beautifully demonstrated in the characterization of the giant

monostratified ganglion cells, that make up a fraction of a percent of the total ganglion cells yet project to multiple central targets and transmit unique signals appropriate to entrain circadian rhythms, drive the pupillary light reflex and perhaps contribute to color processing.

Finally, Table 1 clearly reveals the gaps in the current picture of the morphology, physiology and central projections of macaque ganglion cell types. Surprisingly, it seems to be more the rule than the exception that distinct ganglion cell populations exist at very low densities – 1-5% of the total. The fundamental goal must be to complete the identification and description of the ganglion cell populations by making tracer injections into remaining retinal target structures and to characterize ganglion cell morphology and ultimately their detailed light evoked responses. From what has been learned so far about the existence of multiple cone-opponent pathways and the melanopsin-containing photoreceptive pathway, these low density cell populations will prove to reveal much about the way the retina contributes to the visual process.

Figure Legends

Figure 1. Primate visual pathways. The primate retina projects to at least 15 histologically distinct brainstem sites (Kaas & Huerta, 1988) (O'Brien et al., 2001). Retinorecipient nuclei in the hypothalamus, dorsal and ventral thalamus, and the midbrain are illustrated here semi-schematically, reconstructed from Nissl stained coronal sections through the macaque brain (Paxinos et al., 2000). The optic tract projects the contralateral visual hemifield via crossed nasal and uncrossed temporal ganglion cell axons to seven major brainstem targets: the suprachiasmatic nucleus (SCN) of the hypothalamus at the level of the optic chiasm, the lateral geniculate nucleus (LGN) of the dorsal thalamus, the pregeniculate nucleus (PGN) of the ventral thalamus forming a thin, dorsal 'cap' over the rostral pole of the LGN; a component of the inferior pulvinar, medial subdivision (IPm), situated at the caudomedial pole of the LGN, the pretectal area (PT) at the thalamic-midbrain juncture, and the superior colliculus (SC) and accessory optic system (AOS) of the midbrain. The AOS and PT are further subdivided into distinctive nuclei. The dorsal (DTN), lateral (LTN) and medial (MTN) terminal nuclei of the AOS are retinorecipent outposts linked by a separate optic fascicle that courses around the lateral surface of the midbrain. The nucleus of the optic tract (NOT),

anterior pretectal (APT), olivary pretectal (OPN), posterior pretectal (PPT) nuclei of the pretectal area are spatially intimate but histologically distinct nuclei situated along the course of the optic fibers at the rostrolateral pole of the superior colliculus. In addition the LGN is a complex, laminated structure subdivided into magnocellular (M), parvocellular (P) and koniocellular retinorecipient layers. The retinorecipient zone of the superior colliculus is also a complex layered structure: the stratum zonale (SZ), superficial gray layer (SGS), and the stratum opticum (SO) are all potential zones of input from distinct ganglion cell populations.

Figure 2: High to moderate density ganglion cell populations that project to the LGN (A) Tracings of HRP-stained parasol, small bistratified, and midget cells illustrate dendritic morphology and the difference in dendritic field size of cells near the fovea (small tracings) and peripheral cells (larger tracings). Parasol cells project to the magnocellular layers of the LGN. This ganglion cell class comprises two populations with compact, highly branched trees, narrowly monostratified at ~35% (outer, OFF-center type) and ~65% (inner, ON-center type) depth of the inner plexiform layer (IPL); parasol cells also project to the superior colliculus. Each parasol type is estimated to make up 5-8% of the total ganglion cell population. The small bistratified ganglion cell type composes

a single population estimated at ~6 % of the total and has a dendritic field diameter range similar to that of the parasol ganglion cells. The precise LGN terminus for this cell group is not well established but current evidence suggests a projection to ventral P3 and/or to neighboring koniocellular layer K3. Small bistratified ganglion cells have a more sparsely branching dendritic tree that occupies two narrow strata at 25% and 80% depth in the IPL. Midget ganglion cells project to the parvocellular LGN layers and also comprise two populations with densely branched dendritic trees that stratify broadly at ~10-25% (outer, OFF-center type) and ~75-90% (inner, ON-center type) depth of the IPL. Midget ganglion cells are present at a relative high density, with each type composing ~25% of the total ganglion cells. Schematic cross section of the LGN shows the target lamina of these three cell types. Dendritic field size increases with increasing distance from the fovea, as shown in the plot on the right. (B) Intracellular responses of a parasol, small bistratified, and midget cell to red and green lights modulated in phase (luminance; L and M cones modulated in phase, L cones modulated at ~twice the depth of M cones; traces on the left), red and green lights modulated in counterphase (isoluminance; L cones modulated at ~twice the depth of M cones, middle traces), and to an S-cone isolating stimulus (~80% S-cone contrast, 0% L and M cone contrast; stimulus contrast = traces on the right). Stimulus time course is

shown above each column. Stimulus frequency was 10 Hz for the parasol cell, 4 Hz for the small bistratified cell, and 3.3 Hz for the midget cell. Spike histograms (impulses per second) are shown beneath each voltage trace. This parasol cell showed summed excitatory L and M cone input and had a response minimum at isoluminance, with no significant response to S-cone modulation. The midget ganglion responded to both luminance modulation and at isoluminance, with no response to S-cone modulation. Responses of both parasol and midget ganglion cells, at least in retinal periphery show variable responses to chromatic stimuli that is likely related to variability in the relative weights of L and M cone input to an individual receptive field (see text for further discussion). The small bistratified cell show a strong ON response to S-cone modulation and OFF response to luminance modulation.

Figure 3: In vitro photodynamic staining reveals the detailed dendritic morphology of ganglion cells after retrograde labeling from tracer injections into retinorecipient structures. (A-D) Sequence of photomicrographs showing the progress of photostaining in vitro that was initiated by a brief light exposure. Plane of focus is in the IPL on the dendritic tree of a parasol ganglion cell retrogradely labeled from injections of rhodamine-dextran into the LGN. (A) Tracer initially appears as small bright granules in the soma and dendrites. Upon exposure to light, the granules burst

and release the fluorescent tracer, which diffuses throughout the cytoplasm. Here photostaining has already begun in the soma, which is brightly and uniformly labeled; tracer in the dendrites still appears as small bright granules. Area indicated by the box is enlarged in the inset and a single granule is indicated by the arrow. (B) Photostaining has begun in the dendrites; some granules have burst and tracer is beginning to diffuse through the dendrites. The tracer granule indicated by the arrow in the inset has not yet burst. (C) Photostaining continues as more granules burst and release tracer into the dendrites. (D) Photostaining is complete. Note that the granule indicated by the arrow in the insets has now burst. The entire dendritic tree is uniformly tracer labeled. Photostaining can be used to efficiently characterize the morphology of a large number of retrogradely labeled ganglion cells and also to selectively target individual morphological types in vitro for physiological analysis (Dacey et al., 2003) Scale bar = 50 μm; inset scale bar = 10 μm.

Figure 4. Diverse ganglion cell types with large dendritic field diameters and low to very low relative densities, revealed by retrograde photostaining (Dacey et al., 2003) . Thus far 11 distinctive dendritic morphologies composing up to 17 distinct ganglion cell populations have been identified by retrograde labeling from rhodamine-dextran tracer injections made into LGN,

superior colliculus, and pretectum. (A) Photomicrographs at top illustrate morphological detail observed after retrograde tracer transport that permits cell type identification. Relative dendritic field sizes in retinal periphery are indicated by the disc that surrounds drawings of dendritic morphology observed in retinal flat-mounts. Tracer injections suggest that midget, and small and large bistratified ganglion cells project exclusively to the LGN; parasol, thorny, smooth, sparse, and giant sparse are retrogradely labeled from tracer injection in LGN and superior colliculus. Thus far the recursive monostratified and recursive bistratified groups have been labeled only after tracer injection into the superior colliculus. Depth of dendritic stratification in the IPL is estimated as percentage depth with the GCL as 100%. Stratification of giant sparse cells was determined from melanopsin-labeled cells in vertical sections through the retina. Stratification of all other cell types was determined from HRP stained cells in whole mount retina by measuring the relative stratification of neighboring cells of different types with overlapping dendrites. Scale bars = 50 μm (B) Photomicrograph on the left shows a cross section of the retina. The IPL has been magnified on the right to show the relative dendritic stratification of the cells shown in A. The dendritic trees of most ganglion cell types occupy unique, narrow strata in the IPL. The IPL appears to be subdivided into at least 18 narrow bands; each band is 1-2 μm thick and most ganglion

cell dendritic trees, with the exception of the midget and broad thorny types, are restricted to these narrow bands. GCL, ganglion cell layer; IPL, inner plexiform layer; INL, inner nuclear layer; OPL, outer plexiform layer; ONL, outer nuclear layer.

Figure 5: Morphology and relative dendritic field sizes for the ganglion cell types recognized thus far. Tracings were made from HRP stained cells in peripheral retina. The axon collateral-bearing cell was HRP stained following in vitro intracellular injection of Neurobiotin. An axon collateral (arrow) arises from the axon ~1 mm from the soma. The giant sparse cell was also HRP stained following in vitro intracellular injection of Neurobiotin. All other cells were tracer-labeled by retrograde transport of biotinylated rhodamine dextran injections placed in the LGN or superior colliculus. Shaded circles indicate the number of populations for each morphological group. For example, midget and parasol cells each comprise distinct inner and outer cell populations that are represented here by two overlapping circles. The recursive bistratified and recursive monostratified cells are possible correlates of ON-OFF direction selective and ON direction selective cells respectively (see Table 1). As in rabbit retina, they are represented here as comprising 4 (recursive bistratified) and 3 (recursive monostratified) distinct populations.

Figure 6: S-cone spectral opponency is present in a number of distinct ganglion cell populations. For each type, ganglion cell morphology is shown in relation to voltage recording in response to modulation of either the S-cones or the L+M cones in isolation. To the right of each morphological drawing, best fitting difference-of-Gaussian spatial profiles derived from mapping the sign, strength and spatial extent of the S vs. L+M cone input to the receptive field are shown. (A) Large sparse monostratified ganglion cells show L+M ON, S OFF opponent receptive fields; these cells are stratified in the inner, ON portion of the IPL. The source of the inhibitory S cone signal has not been determined. (B) Large bistratified ganglion cells show S ON responses much like that of the S ON small-bistratified ganglion cell illustrated in C, and are likely also to receive direct excitatory input from the S cone bipolar cell. (C) Small bistratified ganglion cells show S ON, L+M OFF opponent receptive fields. (A fourth S-cone opponent type is shown in Figure 7.) Stimulus was a 2Hz square wave modulation shown below each trace; red, green, and blue lights are varied in amplitude to create cone-isolating conditions. Receptive field structure shown in the difference-of-Gaussians model was measured by the spatial frequency response to drifting gratings that modulated either the S cones or the L+M cones in isolation.

Figure 7: Spatial density, morphology, dendritic stratification, and physiology of the melanopsin-containing, photoreceptive ganglion cell type. (A) A tracing of a whole-mount retina reacted with an antibody against melanopsin is shown on the left. Each dot represents the location of an immunoreactive ganglion cell; both macaque and human retina contain ~3000 melansopsin-containing cells. Cell density is highest near the fovea and drops off sharply toward peripheral retina. T, N, S, I, od; temporal, nasal, superior, and inferior retina, and optic disk. Confocal images of melanopsin-containing ganglion cells are shown on the right. Top micrograph shows a patch of peripheral melanopsin-labeled cells in a flatmount retina (scale bar = 100 μm). Lower micrograph is a reconstruction of the dendritic arbors of 2 neighboring alexa fluor-labeled melanopsin-reactive cells (arrows) from confocal images taken in 5 consecutive vertical sections (25 μm thick) through temporal retina ~ 2 mm from the fovea. Retina was counter stained with a nuclear dye (propidium iodide) to visualize the nuclear layers. The dendrites of these cells can be seen to form two narrow strata located at the extreme inner and outer borders of the IPL (scale bar = 50 μm; GCL, ganglion cell layer; IPL, inner plexiform layer; INL, inner nuclear layer.) (B) Tracing of the complete dendritic tree of a photoreceptive ganglion cell recorded from in the in vitro retina, then intracellularly filled with Neurobiotin and processed for HRP histochemistry following tissue

fixation. These cells correspond to the giant, sparse monostratified ganglion cells that can be retrogradely labeled from tracer injections into the superior colliculus. Arrow indicates axon. Scale bar = 200 μm. Voltage response at the right shows a sustained ON response to a 550 nm 2Hz modulation. Time course of the stimulus is shown below the voltage trace. (C) The cell had an L+M ON, S OFF opponent receptive field. The plot on the left gives the spatial frequency response to drifting gratings used to measure the receptive field. Drifting grating stimuli modulated either the L+M cones (gray circles) or S cones (white circles) in isolation. The data was fit with a difference-of-Gaussian receptive field model (solid lines); the two dimensional Gaussian profile for these fits is shown to the right of the plot; r = Gaussian radius. Traces on the right show the voltage responses to L+M and S cone isolating stimuli. (D) Application of APB and CNQX blocked excitatory glutamatergic transmission and revealed a very slow, sustained, intrinsic photoresponse. Stimulus was a 10 second, 550 nm monochromatic light step. (E) Measurements of the intrinsic photoresponse (solid circles) to a series of monochromatic lights over a 3 log unit range of illumination were used to determine spectral sensitivity of the intrinsic light response. The solid black line is the best fitting retinal based pigment nomogram fit to the data, giving a spectral peak at 483 nm. The spectral

sensitivities of S cones, M cones, and L cones (Baylor et al., 1987) are plotted for comparison (solid gray lines).

TABLE 1 Low density ganglion cell types dominate the retinal landscape

The majority of ganglion cell types that have been identified morphologically a present at relatively low densities of 1-3% of the total population. Moderate-density cell populations – reaching 5-6% of the total include the inner and outer parasol and small bistratified types. The midget ganglion cells are an exception with both inner and outer populations at 25% at 7-8 mm from the fovea. Beyond the midget, parasol and small bistratified populations, very little is currently known about the key physiological properties of the remaining types, though most, if not all of these types project to the LGN and/or the superior colliculus, the two major relays for ascending visual pathways to visual cortical areas.

Acknowledgements

Preparation of this chapter was supported by PHS grants EY06678 and EY09625 to the National Eye Institute and RR0166 to the National Primate Research Center at the University of Washington. I thank Beth Peterson and Toni Haun for preparing the illustrations.

Reference List

Abramov, I., & Gordon, J. (1994). Color appearance: On seeing red--or yellow, or green, or blue. Annu.Rev.Psychol., 45, 451-485.

Ahmad, K. M., Klug, K., Herr, S., Sterling, P., & Schein, S. (2003). Cell density ratios in a foveal patch in macaque retina. Vis Neurosci, 20(2), 189-209.

Baylor, D. A., Nunn, B. J., & Schnapf, J. L. (1987). Spectral sensitivity of cones of the monkey *Macaca fascicularis*. J.Physiol.(Lond.), 390, 145-160.

Berson, D. M., Dunn, F. A., & Takao, M. (2002). Phototransduction by retinal ganglion cells that set the circadian clock. Science, 295(5557), 1070-3.

Calkins, D. J. (1999). Synaptic organization of cone pathways in the primate retina. K. R. Gegenfurtner, & L. T. Sharpe Color vision: from genes to perception (pp. 163-80). New York: Cambridge University Press.

Calkins, D. J., Schein, S. J., Tsukamoto, Y., & Sterling, P. (1994). M and L cones in macaque fovea connect to midget ganglion cells by different numbers of excitatory synapses. Nature, 371, 70-72.

Calkins, D. J., Schein, S. J., Tsukamoto, Y., & Sterling, P. (1995). Density of midget and non-midget ganglion cells in macaque fovea. Soc.Neurosci.Abstr., 23, 1257.

Calkins, D. J., & Sterling, P. (1996). Absence of spectrally specific lateral inputs to midget ganglion cells in primate retina. Nature, 381, 613-615.

Calkins, D. J., & Sterling, P. (1999). Evidence that circuits for spatial and color vision segregate at the first retinal synapse. Neuron, 24, 313-321.

Calkins, D. J., Tsukamoto, Y., & Sterling, P. (1998). Microcircuitry and mosaic of a blue-yellow ganglion cell in the primate retina. J.Neurosci., 18, 3373-85.

Dacey, D. M. (1985). Wide-spreading terminal axons in the inner plexiform layer of the cat's retina: Evidence for intrinsic axon collaterals of ganglion cells. J.Comp.Neurol., 242, 247-262.

Dacey, D. M. (1989). Axon-bearing amacrine cells of the macaque

monkey retina. J.Comp.Neurol., 284, 275-293.

Dacey, D. M. (1993a). Morphology of a small-field bistratified ganglion cell type in the macaque and human retina. Vis.Neurosci., 10, 1081-1098.

Dacey, D. M. (1993b). The mosaic of midget ganglion cells in the human retina. J.Neurosci., 13, 5334-5355.

Dacey, D. M. (1994). Physiology, morphology and spatial densities of identified ganglion cell types in primate retina. Higher Order Processes in the Visual System (pp. 12-34). London: Ciba Foundation.

Dacey, D. M. (1996). Circuitry for color coding in the primate retina. Proc.Natl.Acad.Sci.USA, 93, 582-588.

Dacey, D. M. (1999). Primate retina: cell types, circuits and color opponency. Prog Retin Eye Res, 18(6), 737-63.

Dacey, D. M., & Lee, B. B. (1994). The blue-ON opponent pathway in primate retina originates from a distinct bistratified ganglion cell type. Nature, 367, 731-735.

Dacey, D. M., Lee, B. B., Stafford, D. K., Pokorny, J., & Smith, V. C. (1996). Horizontal cells of the primate retina: cone specificity without spectral opponency. Science, 271, 656-659.

Dacey, D. M., & Petersen, M. R. (1992). Dendritic field size and morphology of midget and parasol ganglion cells of the human retina. Proc.Natl.Acad.Sci.USA, 89, 9666-9670.

Dacey DM, Packer OS, Diller LC, Brainard DH, Peterson BB, & Lee BB. (2000). Center surround receptive field structure of cone bipolar cells in primate retina. Vision Res, 40(14), 1801-1811.

Dacey, D., Peterson, B., Robinson, F., & Gamlin, P. (2003). Fireworks in the primate retina: in vitro photodynamics reveals diverse LGN-projecting ganglion cell types. Neuron, 37(1), 15-27.

DeMonasterio, F. M., & Gouras, P. (1975). Functional properties of ganglion cells of the rhesus monkey retina. J.Physiol.(Lond.), 251, 167-195.

Derrington, A. M., Krauskopf, J., & Lennie, P. (1984). Chromatic mechanisms in lateral geniculate nucleus of macaque. J.Physiol.(Lond.), 357, 219-240.

DeValois, R. L., Abramov, I., & Jacobs, G. H. (1966). Analysis of response patterns of LGN cells. J Opt Soc Am A, 56, 966-977.

DeValois, R. L., Cottaris, N. P., Elfar, S. D., Mahon, L. E., & Wilson, J. A. (2000). Some transformations of color information from lateral geniculate nucleus to striate cortex. Proc.Natl.Acad.Sci.USA, 97(9), 4997-5002.

DeValois, R. L., Cottaris, N. P., Mahon, L. E., Elfar, S. D., & Wilson, J. A. (2000). Spatial and temporal receptive fields of geniculate and cortical cells and directional selectivity. Vision Res, 40(27), 3685-702.

DeValois, R. L., DeValois, K. K., & Mahon, L. E. (2000). Contribution of S opponent cells to color appearance. Proc.Natl.Acad.Sci.USA, 97(1), 512-517.

Diller LC, Packer OS, Verweij J, McMahon MJ, Williams DR, & Dacey DM. (in press). L- and M-cone contributions to the midget and parasol ganglion cell receptive fields of macaque monkey retina. J Neurosci.

Famiglietti, E. V., Kaneko, A., & Tachibana, M. (1977). Neuronal architecture of on and off pathways to ganglion cells in carp retina. Science, 198, 1267-1269.

Foster, R. G. & Helfrich-Forster, C. (2001). The regulation of circadian clocks by light in fruitflies and mice. Philos Trans R Soc Lond B Biol Sci, 356 (1415), 1779-89.

Gamlin, P. D., Zhang, H., Harlow, A., & Barbur, J. L. (1998). Pupil responses to stimulus color, structure and light flux increments in the rhesus monkey. Vision Res, 38(21), 3353-8.

Gamlin, P. D., Zhang, H. Y., & Clarke, R. J. (1995). Luminance neurons in the pretectal olivary nucleus mediate the pupillary light reflex in the rhesus monkey. Exp.Brain Res., 106, 177-180.

Gamlin PDR, Peterson BB, & Dacey DM. (2001). Physiology and morphology of retinal ganglion cells projecting to the pretectal olivary nucleus of the rhesus monkey. Vol. 42(4), S676.

Gegenfurtner, K. R. & Kiper, D. C. (2003) Color vision. Ann. Rev. Neurosci. 26, 181-206

Hendry, S. H. C. & Reid, R. C. (2000). The koniocellular pathway in primate vision. Annu.Rev.Neurosci. 23, 127-53.

Isayama, T., Berson, D. M., & Pu, M. (2000). Theta ganglion cell type of cat retina. J.Comp.Neurol., 417(1), 32-48.

Jacobs, G. H. (1993). The distribution and nature of colour vision among the mammals. Biol.Rev.Camb.Philos.Soc., 68, 413-471.

Jacobs, G. H., & Deegan, J. F.2nd. (1997). Spectral sensitivity of macaque monkeys measured with ERG flicker photometry. Vis.Neurosci., 14, 921-928.

Jacoby, R. A., & Marshak, D. W. (2000). Synaptic connections of DB3 diffuse bipolar cell axons in macaque retina. J.Comp.Neurol., 416(1), 19-29.

Jacoby, R. A., Wiechmann, A. F., Amara, S. G., Leighton, B. H., & Marshak, D. W. (2000). Diffuse bipolar cells provide input to OFF parasol ganglion cells in the macaque retina. J.Comp.Neurol., 416(1), 6-18.

Kaas, J. H., & Huerta, M. F. (1988). The subcortical visual system of primates. Comparative Primate Biology, Vol. 4 : Neurosciences (pp. 327-391). Alan R. Liss, Inc.

Kaplan, E., Lee, B. B., & Shapley, R. M. (1990). New views of primate retinal function. Prog Retin Eye Res, 9, 273-336.

Kaplan, E., & Shapley, R. M. (1982). X and Y cells in the lateral geniculate nucleus of macaque monkeys. J. Physiol. (Lond), 330, 125-143.

Kaplan, E., & Shapley, R. M. (1986). The primate retina contains two types of ganglion cells, with high and low contrast sensitivity. Proc.Natl.Acad.Sci.USA, 83, 2755-2757.

Klug, K., Tsukamoto, Y., Sterling, P., & Schein, S. (1993). Blue cone off-midget ganglion cells in macaque. Vol. 34(4), 986.

Knoblauch, K., & Shevell, S. K. (2001). Relating cone signals to color appearance: failure of monotonicity in yellow/blue. Vis Neurosci, 18(6), 901-6.

Kolb, H., & Dekorver, L. (1991). Midget ganglion cells of the parafovea of the human retina: A study by electron microscopy and serial section reconstructions. J.Comp.Neurol., 303, 617-636.

Kolb, H., Linberg, K. A., & Fisher, S. K. (1992). Neurons of the human retina: A Golgi study. J.Comp.Neurol., 318, 147-187.

Kremers, J., Lee, B. B., Pokorny, J., & Smith, V. C. (1993). Responses of macaque ganglion cells and human observers to compound periodic waveforms. Vision Res., 33, 1997-2011.

Lee, B. B. (1991). On the relation between cellular sensitivity and psychophysical detection. A. Valberg, & B. B. Lee From Pigments to Perception (pp. 105-113). New York: Plenum Press.

Lee, B. B. (1999). Receptor inputs to primate ganglion cells. K. R. Gegenfurtner, & L. T. Sharpe Color vision: from genes to perception (pp. 203-18). New York: Cambridge University Press.

Lennie, P. (2000). Color vision: putting it together. Curr Biol, 10(16), R589-91.

Leventhal, A. G., Rodieck, R. W., & Dreher, B. (1981). Retinal ganglion cell classes in the old world monkey: Morphology and central projections. Science, 213, 1139-1142.

Lynch, J. J. I., Silveira, L. C. L., Perry, V. H., & Merigan, W. H. (1992). Visual effects of damage to P ganglion cells in macaques. Vis.Neurosci., 8, 575-583.

Marshak, D. W., Yamada, E. S., Bordt, A. S., & Perryman, W. C. (2002). Synaptic input to an ON parasol ganglion cell in the macaque retina: a serial section analysis. Vis Neurosci, 19(3), 299-305.

Martin, P. R., Lee, B. B., White, A. J., Solomon, S. G., & Ruttiger, L. (2001). Chromatic sensitivity of ganglion cells in the peripheral primate retina. Nature, 410(6831), 933-6.

Martin, P. R., White, A. K., Wilder, H. D., Y Sefton, A. E. (1997). Evidence that blue-on cells are part of the third geniculocortical pathway in primates. Eur.J.Neurosci., 9(7), 1536-41.

Masland, R. H. (2001). Neuronal diversity in the retina. Curr Opin Neurobiol, 11(4), 431-6.

Masland, R. H., & Raviola, E. (2000). Confronting complexity: strategies for understanding the microcircuitry of the retina. Annu Rev Neurosci, 23, 249-84.

McMahon, M. J., Lankheet, M. J. M., Lennie, P., & Williams, D. R. (2000). Fine structure of parvocellular receptive fields in the primate fovea revealed by laser interferometry. J.Neurosci., 20(5), 2043-2053.

Merigan, W. H. (1989). Chromatic and achromatic vision of macaques: role of the P pathway. J.Neurosci., 9, 776-783.

Merigan, W. H. (1996). Basic visual capacities and shape discrimination after lesions of extrastriate area V4 in macaques. Vis.Neurosci., 13, 51-60.

Merigan, W. H., Byrne, C. E., & Maunsell, J. H. R. (1991a). Does primate motion perception depend on the magnocellular pathway. J.Neurosci., 11, 3422-3429.

Merigan, W. H., Katz, L. M., & Maunsell, J. H. (1991b). The effects of parvocellular lateral geniculate lesions on the acuity and contrast sensitivity of macaque monkeys. J Neurosci, 11(4), 994-1001.

Merigan, W. H., & Maunsell, J. H. (1990). Macaque vision after magnocellular lateral geniculate lesions. Vis Neurosci, 5(4), 347-52.

Merigan, W. H., & Maunsell, J. H. R. (1993). How parallel are the primate visual pathways. Annu.Rev.Neurosci., 16, 369-402.

Monnier, P., & Shevell, S. K. (2003). Large shifts in color appearance from patterned chromatic backgrounds. Nat Neurosci, 6(8), 801-802.

Neitz M, & Neitz J. (2003). Molecular genetics of human color vision and color vision defects. Chalupa LM, & Werner JS (editors), The Visual Neurosciences .

O'Brien, B. J., Abel, P. L., & Olavarria, J. F. (2001). The retinal input to calbindin-D28k-defined subdivisions in macaque inferior pulvinar. Neurosci Lett, 312(3), 145-8.

Packer, O. S., & Williams, D. R. (2003) Light, retinal imagery and photoreceptors. S. Shevell The Science of Color (p. 41-102).

Paxinos G, Huang X-F, & Toga AW. (2000). The rhesus monkey brain in stereotaxic coordinates. San Diego CA: Academic Press.

Peichl, L., Ott, H. and Boycott, B. B. (1987) Alpha ganglion cells in mammalian retina. Proc. R. Soc. Lond. B Biol.

Sci., 231, 169-197.

Perry, V. H., & Cowey, A. (1984). Retinal ganglion cells that project to the superior colliculus and pretectum in the macaque monkey. Neuroscience, 12(4), 1125-1137.

Perry, V. H., Oehler, R., & Cowey, A. (1984). Retinal ganglion cells that project to the dorsal lateral geniculate nucleus in the macaque monkey. Neuroscience, 12(4), 1101-1123.

Peterson, B. B., & Dacey, D. M. (1998). Morphology of human retinal ganglion cells with intraretinal axon collaterals. Vis Neurosci, 15(2), 377-87.

Peterson, B. B., & Dacey, D. M. (1999). Morphology of wide-field, monostratified ganglion cells of the human retina. Vis Neurosci, 16(1), 107-20.

Peterson, B. B., & Dacey, D. M. (2000). Morphology of wide-field bistratified and diffuse human retinal ganglion cells. Vis Neurosci, 17(4), 567-78.

Polyak, S. L. (1941). The Retina. Chicago: University of Chicago Press.

Reid, R. C., & Shapley, R. M. (2002). Space and time maps of cone photoreceptor signals in macaque lateral geniculate nucleus. J Neurosci, 22(14), 6158-75.

Rockhill, R. L., Daly, F. J., MacNeil, M. A., Brown, S. P., & Masland, R. H. (2002). The diversity of ganglion cells in a mammalian retina. J Neurosci, 22(9), 3831-43.

Rodieck, R. W. (1991). Which cells code for color? A. Valberg, & B. B. Lee From Pigments to Perception (pp. 83-93). New York: Plenum Press.

Rodieck, R. W. (1998). The First Steps in Seeing. Sunderland MA: Sinauer Associates, Inc.

Rodieck, R. W., Binmoeller, K. F., & Dineen, J. (1985). Parasol and midget ganglion cells of the human retina. J.Comp.Neurol., 233, 115-132.

Rodieck, R. W., Brening, R. K. & Watanabe, M. (1993) The origin of parallel visual pathways. R. Shapley and D. M.-K. Lam Contrast Sensitivity (pp. 117-144). Cambridge: MIT press

Rodieck, R. W., & Watanabe, M. (1993). Survey of the morphology of macaque retinal ganglion cells that project to the

pretectum, superior colliculus, and parvicellular laminae of the lateral geniculate nucleus. J.Comp.Neurol., 338, 289-303.

Roorda, A., Metha, A. B., Lennie, P., & Williams, D. R. (2001). Packing arrangement of the three cone classes in primate retina. Vision Res., 41(10-11), 1291-1306.

Roorda, A., & Williams, D. R. (1999). The arrangement of the three cone classes in the living human eye [see comments]. Nature, 397(6719), 520-2.

Schnapf, J. L., Kraft, T. W., & Baylor, D. A. (1987). Spectral sensitivity of human cone photoreceptors. Nature, 325, 439-441.

Shapley, R. (1995). Parallel neural pathways and visual function. M. S. Gazzaniga, E. Bizzi, I. B. Black, C. Blakemore, L. Cosmides, S. M. Kosslyn, J. E. LeDoux, J. A. Movshon, S. Pinker, M. I. Posner, P. Rakic, D. L. Schacter, J. Tooby, & E. Tulving The Cognitive Neurosciences (1 ed., pp. 315-324). Cambridge: MIT Press.

Shapley, R., & Perry, V. H. (1986). Cat and monkey retinal ganglion cells and their visual functional roles. Trends Neurosci., 9, 229-235.

Silveira, L. C. L., & Perry, V. H. (1991). The topography of magnocellular projecting ganglion cells (M-ganglion cells) in the primate retina. Neuroscience, 40, 217-237.

Sterling, P. (1998). Retina - (4th edition). G. M. Shepherd The Synaptic Organization of the Brain (4 ed., pp. 205-253). New York: Oxford University Press.

Sun, W., Li, N. & He, S. (2002). Large scale morphological survey of mouse retinal ganglion cells. J. Comp. Neurol. 451, 115-126.

Vaney, D. I., Peichl, L., Wassle, H., & Illing, R. B. (1981). Almost all ganglion cells in the rabbit retina project to the superior colliculus. Brain Res, 212, 447-53.

Vaney, D., He, S., Taylor, W., & Levick, W. (2000). Direction-selective ganglion cells in the retina. J. Zanker, & Zeil Computational, neural and ecological constraints of visual motion processing . Berlin: Springer Verlag.

Wässle, H. (1999). Parallel pathways from the outer to the inner

retina in primates. K. R. Gegenfurtner, & L. T. Sharpe Color vision: from genes to perception (pp. 145-62). New York: Cambridge University Press.

Wässle, H., & Boycott, B. B. (1991). Functional architecture of the mammalian retina. Physiol.Rev., 71, 447-480.

Wässle, H., Grünert, U., Röhrenbeck, J., & Boycott, B. B. (1990). Retinal ganglion cell density and cortical magnification factor in the primate. Vision Res., 30, 1897-1911.

Watanabe, M., & Rodieck, R. W. (1989). Parasol and midget ganglion cells of the primate retina. J.Comp.Neurol., 289, 434-454.

Wiesel, T. N., & Hubel, D. H. (1966). Spatial and chromatic interactions in the lateral geniculate body of the rhesus monkey. J.Neurophysiol., 29, 1115-1156.

Zhang, H. Y., Clarke, R. J., & Gamlin, P. D. R. (1996). Behavior of luminance neurons in the pretectal olivary nucleus during the pupillary near response. Exp.Brain Res., 112, 158-162.

Table 1
Summary of ganglion cell types in macaque retina

	Ganglion cell morphological type	% of total ganglion cell population*	Central projections	Some physiological properties
1	Midget Inner	26%	LGN parvo 5, 6	ON-center; OFF-surround Achromatic/chromatic L vs M cone opponent
2	Midget Outer	26%	LGN parvo 3, 4	OFF center; ON surround Achromatic/chromatic L vs M cone opponent S cone OFF opponent group?
3	Parasol Inner	8.0%	LGN magno 1, 2	ON-center; OFF-surround Achromatic L+M cone input S cone input controversial
4	Parasol Outer	8.0%	LGN magno 1, 2	OFF-center; ON-surround Achromatic L+M cone input S cone input controversial
5	Small bistratified	6.2%	LGN konio 3	S ON; L+M OFF opponent
6	Large bistratified	2.7%	LGN	S ON opponent details unknown
7	Thorny monostratified Inner	1.2%	LGN Superior colliculus	Unknown
8	Thorny monostratified Outer	1.2%	LGN Superior colliculus	Unknown
9	Broad thorny monostratified	1.2%	LGN Superior colliculus	Unknown
10	Recursive bistratified	4.2%	Superior colliculus	Possible correlate of ON-OFF direction selective
11	Recursive monostratified	1.9%	Superior colliculus LGN? Pretectal area (NOT?)	Possible correlate of ON direction selective
12	Moderate monostratified Inner	1.3%	Superior colliculus	Unknown
13	Moderate monostratified Outer	1.3%	Superior colliculus	Unknown
14	Sparse monostratified Inner	2.0 %	LGN	L+M ON; S OFF opponent
15	Sparse monostratified Outer	1.2%	LGN	Unknown
16	Giant monostratified Melanopsin-containing Inner/outer Weakly bistratified	1.0%	LGN Pretectal area, PON SCN?	Sustained ON response S OFF; L+M ON opponent Strong rod input Intrinsically photosensitive via novel photopigment
17	Giant monostratified intrinsic axon-collaterals	1.0%	Unknown	Unknown

*Total ganglion cell density is from Wässle et al., 1989, for temporal retina ~ 8 mm from the fovea. Individual cell type densities were determined from cell density at ~8 mm (parasol cells, Perry & Cowey, 1985) or from dendritic field area at ~ 8 mm and coverage factor where known (thorny and giant monostratified cells, Dacey, unpublished; midget cells Dacey, 1993). All other cell type densities were determined from measured dendritic field area at ~8 mm and estimated coverage. For abbreviations, see Figure 1.

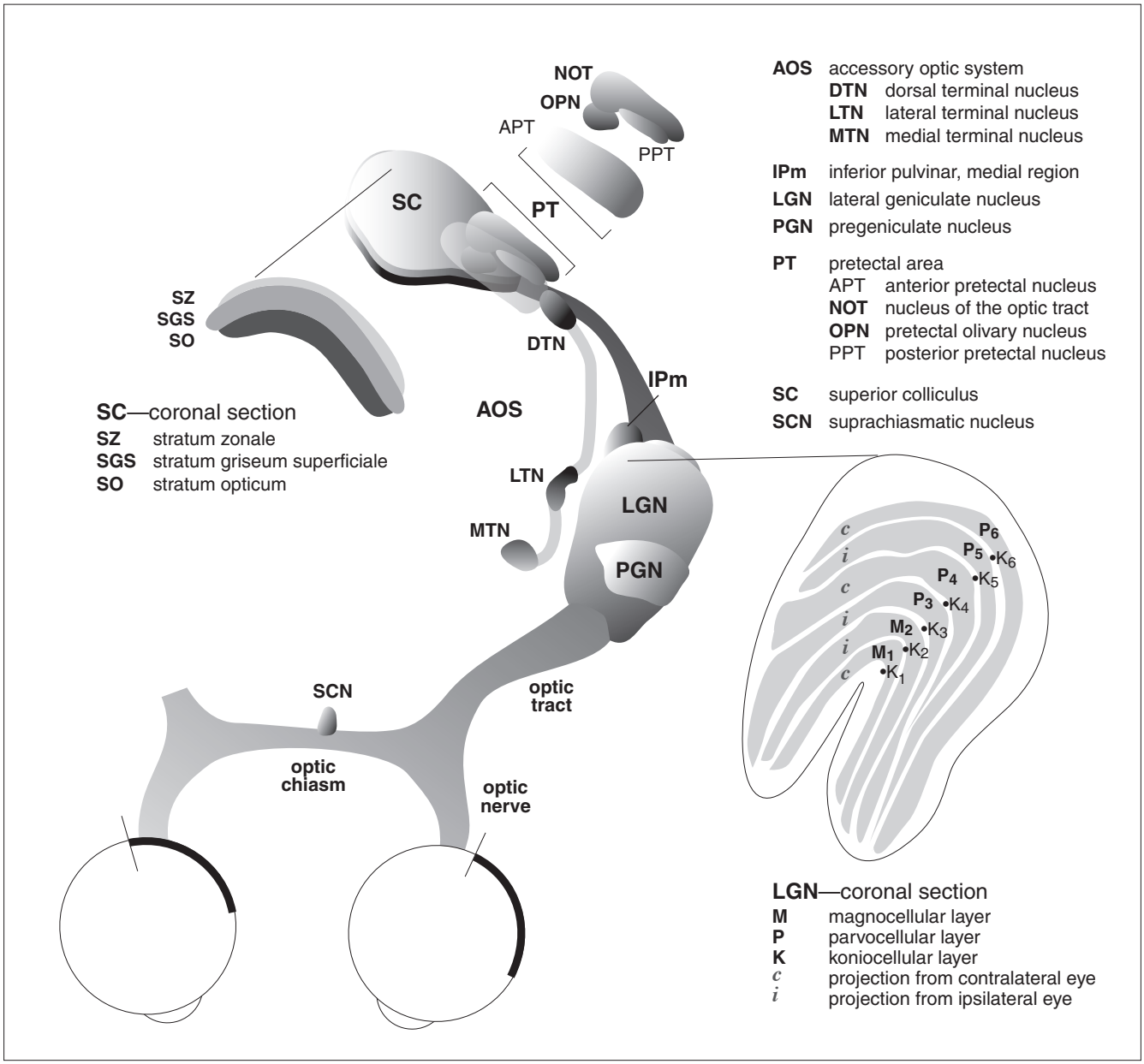
NOT
OPN
APT
PPT
SC
PT
SZ
SGS
SO
DTN
IPm
AOS
LTN
LGN
MTN
PGN
SCN
optic tract
optic chiasm
optic nerve
SC—coronal section
SZ stratum zonale
SGS stratum griseum superficiale
SO stratum opticum
AOS accessory optic system
DTN dorsal terminal nucleus
LTN lateral terminal nucleus
MTN medial terminal nucleus
IPm inferior pulvinar, medial region
LGN lateral geniculate nucleus
PGN pregeniculate nucleus
PT pretectal area
APT anterior pretectal nucleus
NOT nucleus of the optic tract
OPN pretectal olivary nucleus
PPT posterior pretectal nucleus
SC superior colliculus
SCN suprachiasmatic nucleus
c
i
c
i
i
c
P6
P5 •K6
P4 •K5
P3 •K4
M2 •K3
M1 •K2
•K1
LGN—coronal section
M magnocellular layer
P parvocellular layer
K koniocellular layer
c projection from contralateral eye
i projection from ipsilateral eye

Figure 1

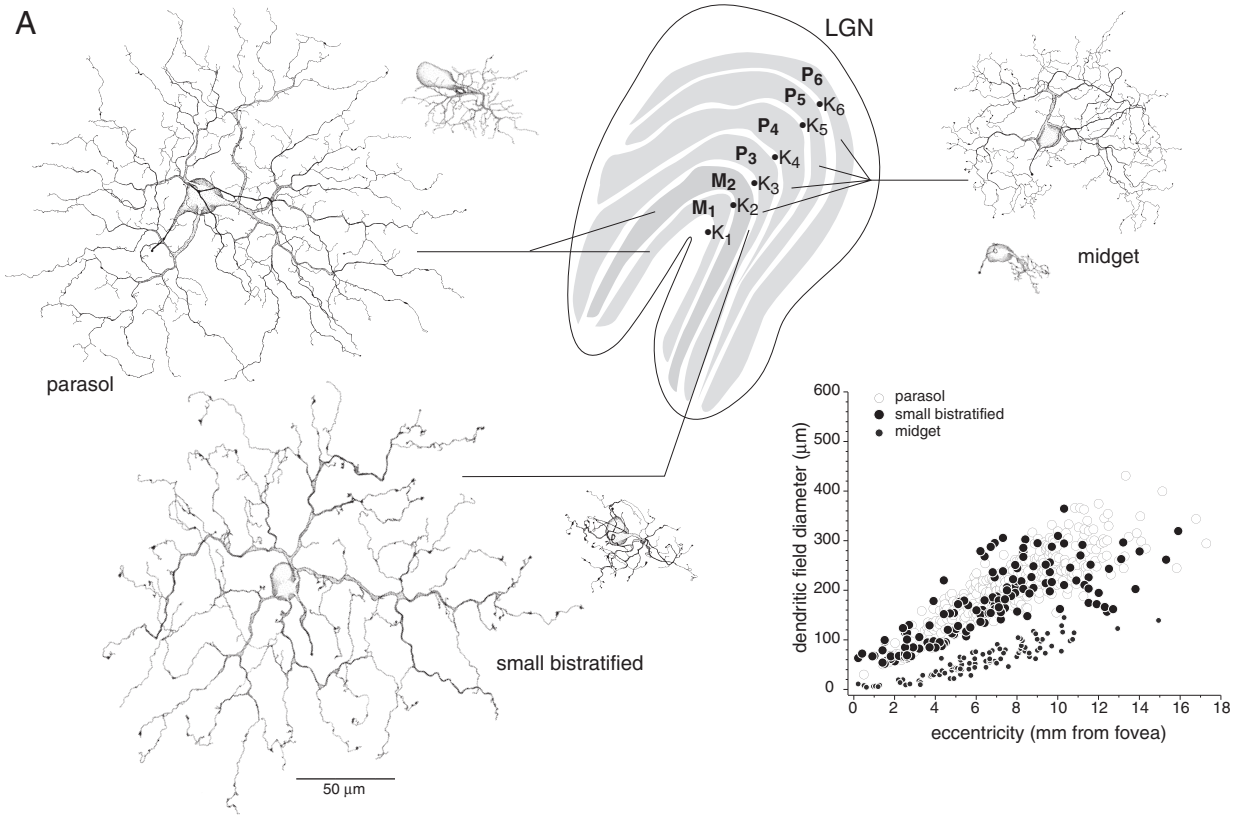
A
LGN
P6
P5
K6
P4
K5
P3
K4
M2
K3
M1
K2
K1
midget
parasol
small bistratified
50 µm
parasol
small bistratified
midget
dendritic field diameter (µm)
eccentricity (mm from fovea)

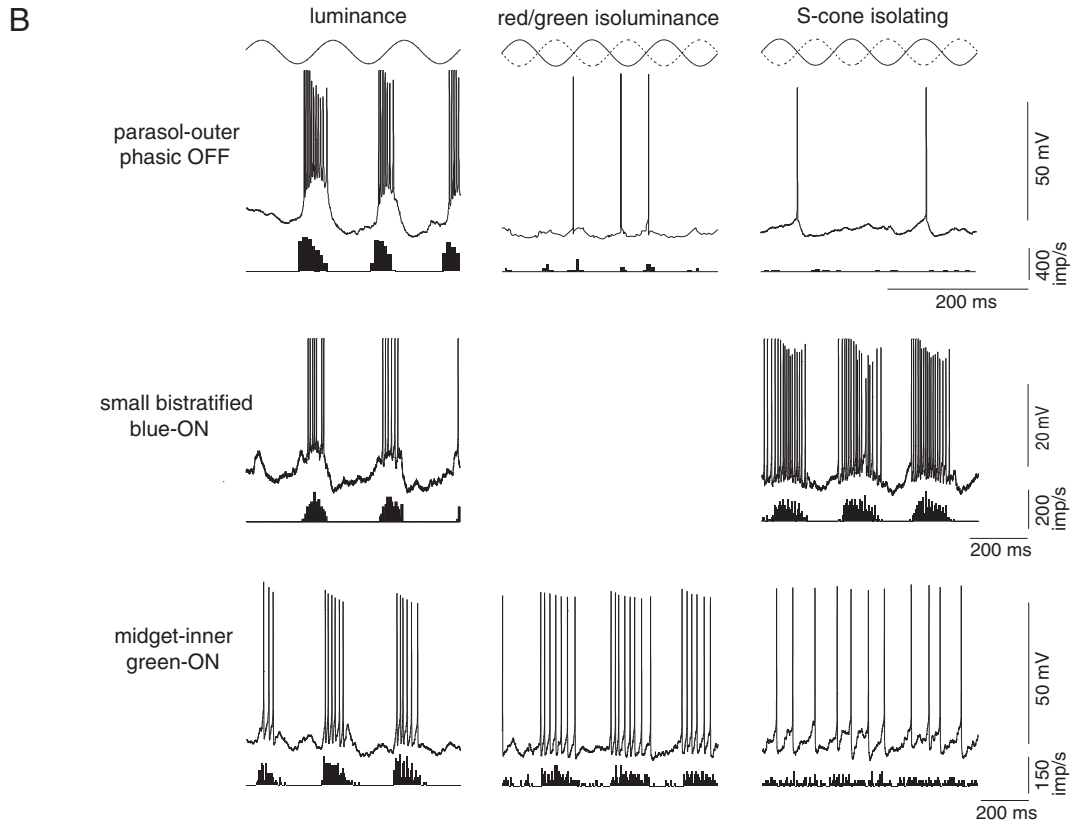
B
luminance
red/green isoluminance
S-cone isolating
parasol-outer
phasic OFF
50 mV
400
imp/s
200 ms
small bistratified
blue-ON
20 mV
200
imp/s
200 ms
midget-inner
green-ON
50 mV
150
imp/s
200 ms

Figure 2

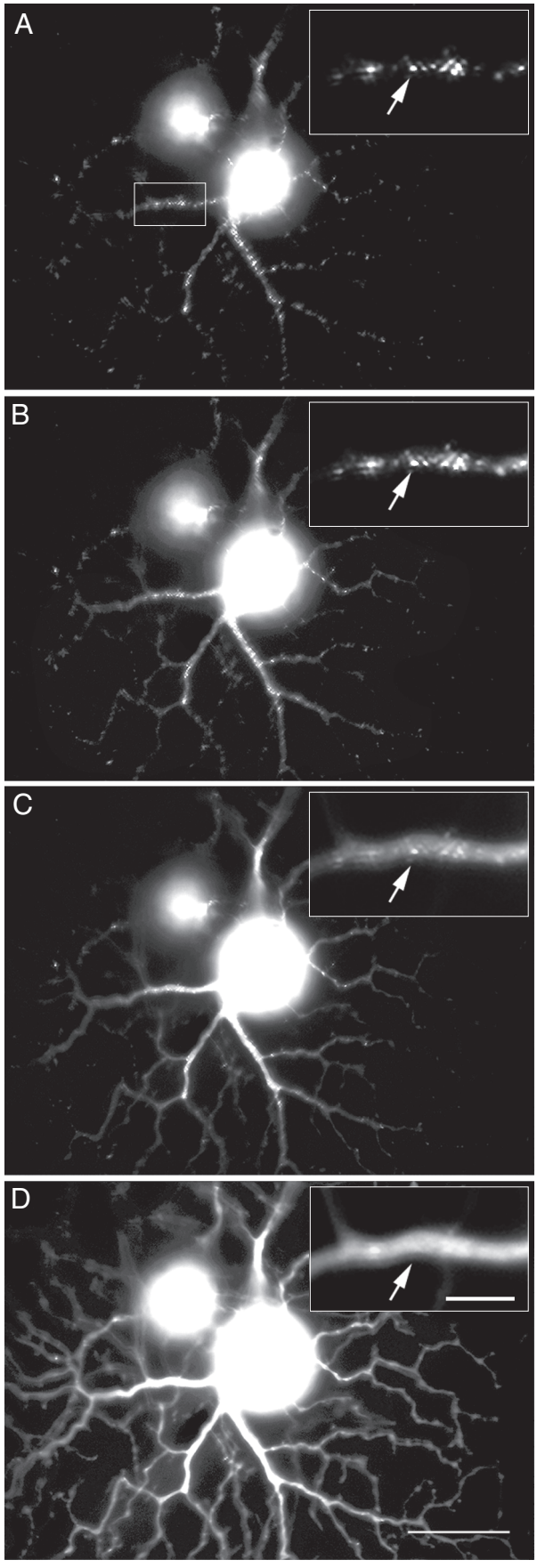

Figure 3

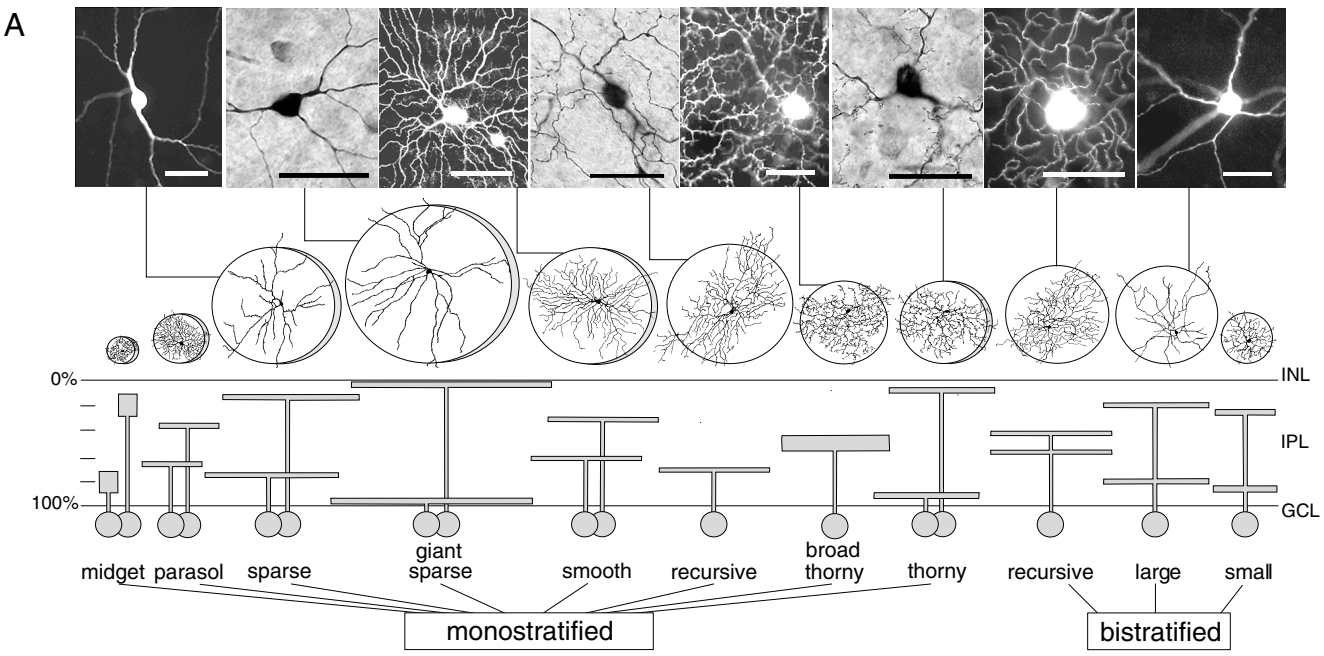
A
0%
100%
INL
IPL
GCL
midget
parasol
sparse
giant sparse
smooth
recursive
broad thorny
thorny
recursive
large
small
monostratified
bistratified

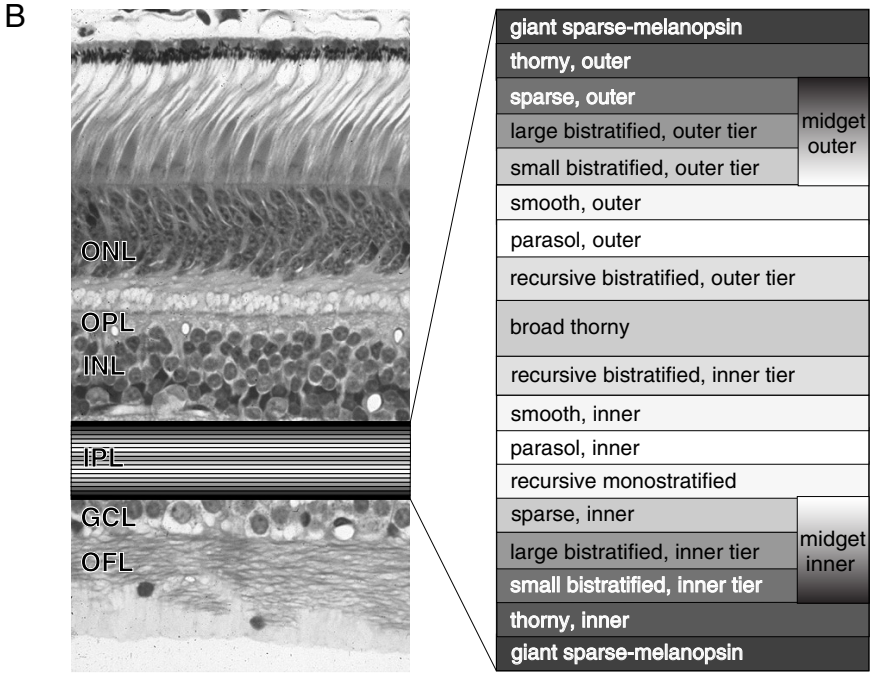
B
ONL
OPL
INL
IPL
GCL
OFL
giant sparse-melanopsin
thorny, outer
sparse, outer
large bistratified, outer tier
small bistratified, outer tier
midget outer
smooth, outer
parasol, outer
recursive bistratified, outer tier
broad thorny
recursive bistratified, inner tier
smooth, inner
parasol, inner
recursive monostratified
sparse, inner
large bistratified, inner tier
small bistratified, inner tier
midget inner
thorny, inner
giant sparse-melanopsin

Figure 4

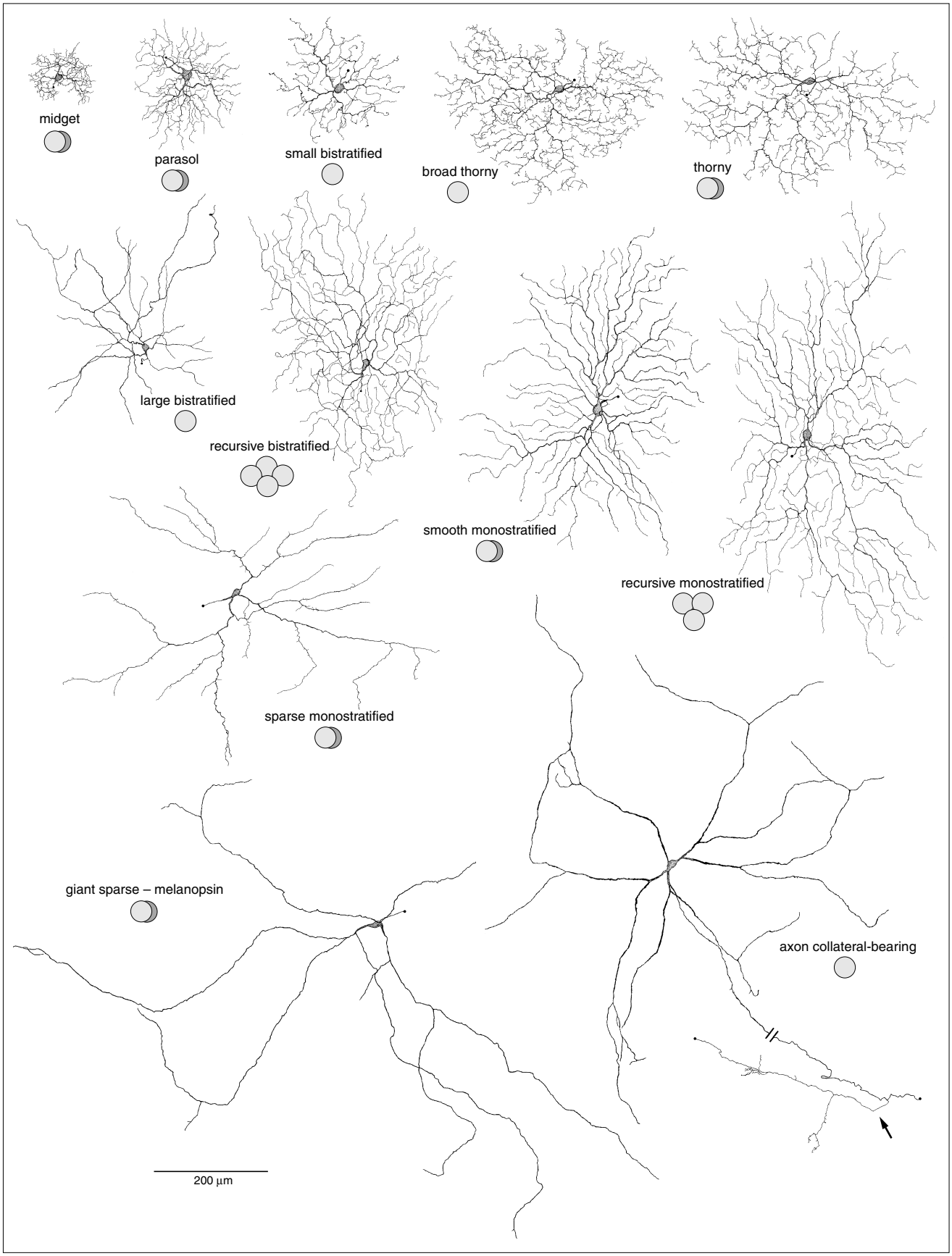
midget
parasol
small bistratified
broad thorny
thorny
large bistratified
recursive bistratified
smooth monostratified
recursive monostratified
sparse monostratified
giant sparse – melanopsin
axon collateral-bearing
200 µm

Figure 5

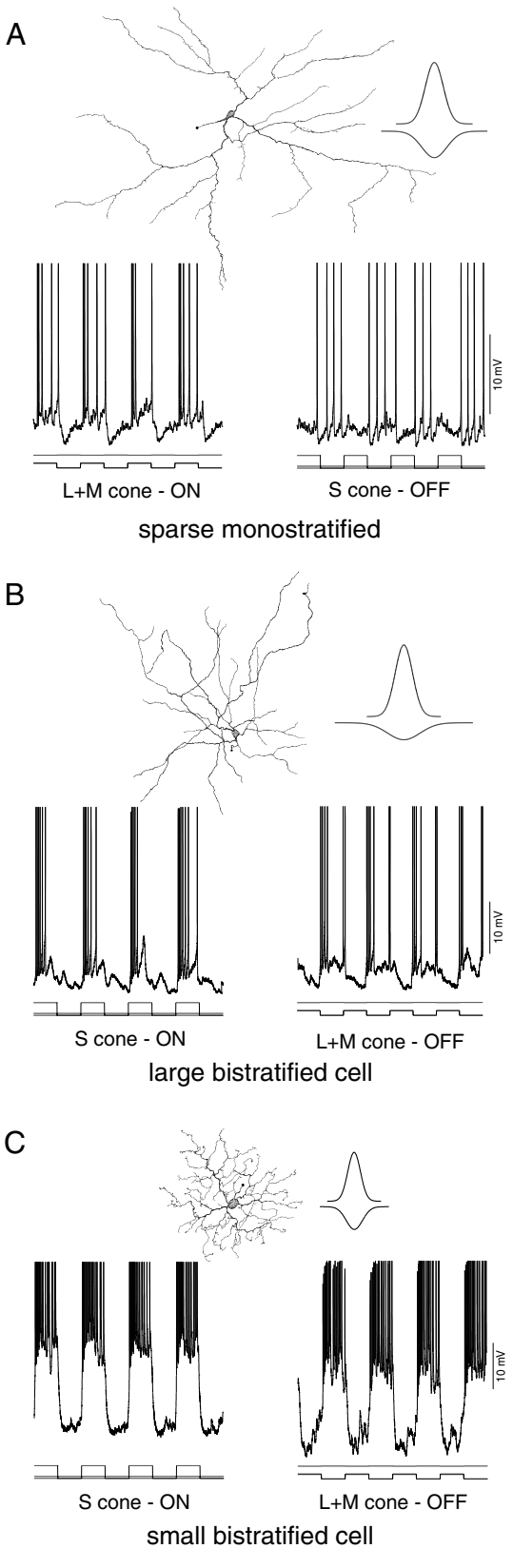
A
10 mV
L+M cone - ON
S cone - OFF
sparse monostratified
B
10 mV
S cone - ON
L+M cone - OFF
large bistratified cell
C
10 mV
S cone - ON
L+M cone - OFF
small bistratified cell

Figure 6

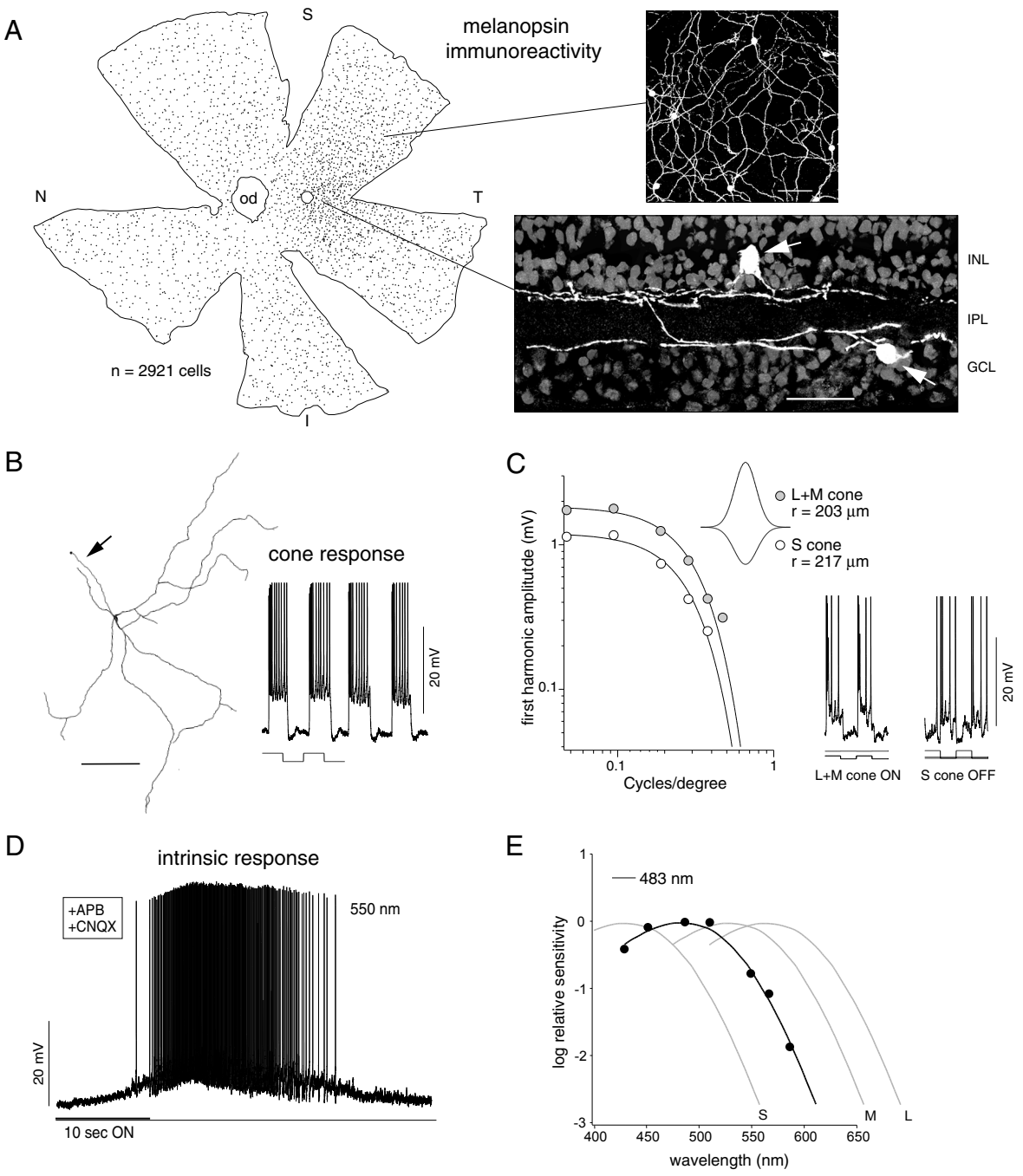
A
S
N
od
T
I
n = 2921 cells
melanopsin
immunoreactivity
INL
IPL
GCL
B
cone response
20 mV
C
L+M cone
r = 203 µm
S cone
r = 217 µm
first harmonic amplitutde (mV)
1
0.1
0.1
1
Cycles/degree
L+M cone ON
S cone OFF
20 mV
D
intrinsic response
+APB
+CNQX
550 nm
20 mV
10 sec ON
E
483 nm
log relative sensitivity
1
0
-1
-2
-3
S
M
L
400
450
500
550
600
650
wavelength (nm)

Figure 7